VU Research Portal

Kohn-Sham potentials and exchange and correlation energy densities from one- and two-electron density matrices for Li2, N2, F2.

Schipper, P.R.T.; Gritsenko, O.V.; Baerends, E.J.

published in
Physical Review A. Atomic, Molecular and Optical Physics
1998

DOI (link to publisher)
10.1103/PhysRevA.57.1729

document version
Publisher's PDF, also known as Version of record

Kohn-Sham potentials and exchange and correlation energy densities from one- and two-electron density matrices for Li_2, N_2, and F_2

P. R. T. Schipper, O. V. Gritsenko, and E. J. Baerends
Scheikundig Laboratorium der Vrije Universiteit, De Boelelaan 1083, 1081 HV Amsterdam, The Netherlands
(Received 27 May 1997)

A definition of key quantities of the Kohn-Sham form of density-functional theory such as the exchange-correlation potential v_{xc} and the energy density ε_{xc} in terms of wave-function quantities (one- and two-electron density matrices) is given. This allows the construction of v_{xc} and ε_{xc} numerically as functions of $\mathbf{r}$ from *ab initio* wave functions. The behavior of the constructed exchange ε_x and correlation ε_c energy densities and the corresponding integrated exchange E_x and correlation E_c energies have been compared with those of the local-density approximation (LDA) and generalized gradient approximations (GGA) of Becke, of Perdew and Wang, and of Lee, Yang, and Parr. The comparison shows significant differences between $\varepsilon_c(\mathbf{r})$ and the $\varepsilon_c^{GGA}(\mathbf{r})$, in spite of some gratifying similarities in shape for particularly ε_c^{PW}. On the other hand, the local behavior of the GGA exchange energy densities is found to be very similar to the constructed $\varepsilon_x(\mathbf{r})$, yielding integrated energies to about 1% accuracy. Still the remaining differences are a sizable fraction ($\sim$25%) of the correlation energy, showing up in differences between the constructed and model exchange energy densities that are locally even larger than the typical correlation energy density. It is argued that nondynamical correlation, which is incorporated in $\varepsilon_c(\mathbf{r})$, is lacking from $\varepsilon_c^{GGA}(\mathbf{r})$, while it is included in $\varepsilon_x^{LDA}(\mathbf{r})$ and $\varepsilon_x^{GGA}(\mathbf{r})$ but not in $\varepsilon_x(\mathbf{r})$. This is verified almost quantitatively for the integrated energies. It also appears to hold locally in the sense that the difference $\varepsilon_x^{GGA}(\mathbf{r})-\varepsilon_x(\mathbf{r})$ may be taken to represent $\varepsilon_c^{nondyn}(\mathbf{r})$ and can be added to $\varepsilon_c^{GGA}(\mathbf{r})$ to bring it much closer to $\varepsilon_c(\mathbf{r})$. [S1050-2947(98)02703-6]

PACS number(s): 31.15.Ew, 31.15.Ar, 31.25.Nj, 31.10.+z

I. INTRODUCTION

Examples of accurate Kohn-Sham (KS) functionals constructed numerically from accurate (*ab initio*) wave functions for chemically interesting systems are of importance for an understanding of the success of density-functional theory (DFT) and for its further development as well as for analysis of the effect of electron correlation [1,2]. It has recently been shown that it is indeed possible to obtain all the key KS quantities such as the exchange-correlation KS potential $v_{xc}([\rho];\mathbf{r})$ [3–8], energy density per particle $\varepsilon_{xc}([\rho];\mathbf{r})$ [9,10], and various energy characteristics from the correlated *ab initio* electron density $\rho(\mathbf{r})$ and the one- and two-electron density matrices.

The energy density ε_{xc} is usually considered to be the most interesting quantity since it directly yields the exchange-correlation energy E_{xc} of a many-electron system through the integral

$$E_{xc}[\rho]=\int \rho(\mathbf{r})\varepsilon_{xc}([\rho];\mathbf{r})d\mathbf{r}. \tag{1.1}$$

Modeling of ε_{xc} with approximate functionals has therefore become an essential part of the development of DFT. The specific expression which the approximate energy density takes as a function of the electron coordinate is, however, not uniquely defined, i.e., the expression can be altered by addition of any functional of the density that integrates to zero over the density. In this respect the uniquely defined exchange-correlation potential v_{xc}, defined through the functional derivative

$$v_{xc}(\mathbf{r})=\frac{\delta E_{xc}[\rho]}{\delta\rho}, \tag{1.2}$$

is a severe test for approximate functionals. Unfortunately, the potentials corresponding to the local-density approximation (LDA) and the current generalized gradient approximations (GGA) do not reproduce essentially accurate potentials particularly well [6,11,12], so that special gradient- and Laplacian-dependent approximations were developed for v_{xc} [6,13]. In spite of the fundamental importance of v_{xc}, however, it is rather the energy density ε_{xc} that is receiving most attention.

Usually, ε_{xc} is further subdivided into the exchange ε_x and correlation ε_c energy densities that yield the corresponding energies E_x and E_c. Approximate functional forms of $\varepsilon_x([\rho];\mathbf{r})$ and $\varepsilon_c([\rho];\mathbf{r})$ are derived from homogeneous or inhomogeneous electron-gas models [14,15] with due account of various scaling and asymptotic properties. The parameters of the approximate functionals can be obtained nonempirically from sum-rule conditions [15] but usually they are fitted to reproduce conventional E_x [16] and E_c [17–19] values for prototype atomic systems. The current GGA functionals obtained in this way provide a surprisingly good description of a number of molecular characteristics, in particular, of the molecular thermochemistry. In many cases the accuracy of the calculated bonding and atomization energies of molecules is approaching conventional ''chemical accuracy'' [20,21].

In spite of the extensive analysis of the GGA functionals performed in the literature, the form of ε_x and ε_c as functions of the electron coordinate $\mathbf{r}$ is seldom taken into consideration and little is still known about the local behavior of

the standard LDA and GGA ε_x and ε_c models. Moreover, for molecules the exchange and correlation energies obtained with these models are seldom compared with the estimates of the true DFT exchange and correlation energies.

In this paper $v_{\rm xc}$ and $\varepsilon_{\rm xc}$ are constructed numerically from *ab initio* one- and two-electron density matrices for the homonuclear diatomic closed-shell molecules Li_2, N_2, and F_2. These molecules are considered as prototype systems with truly covalent bonds and they are included into any representative set of molecules to check the accuracy of approximations in DFT. They represent rather different cases of covalent bonding, ranging from the weakly bonded Li_2 with a single $2s$-based σ bond, to the very strongly bonded N_2 with one σ and two π bonds, to the weakly bonded F_2 with one $2p$-based σ bond and Pauli repulsion between two p_π lone pairs on each F atom.

The paper is organized as follows. Section II contains definitions of the quantities $\varepsilon_{\rm xc}$ and $v_{\rm xc}$ in terms of density matrices. We will show that some physically meaningful contributions to these quantities can be distinguished that clarify the relationship between $\varepsilon_{\rm xc}$ and $v_{\rm xc}$. These are, first, the potential of the exchange-correlation hole $v_{\rm xc}^{\rm hole}$ and the potential $v_{c,\rm kin}$, representing the effect of Coulomb correlation on the kinetic functional. The sum $\frac{1}{2}v_{\rm xc}^{\rm hole}+v_{c,\rm kin}$ represents a physically well motivated choice for the function $\varepsilon_{\rm xc}(\mathbf{r})$ and these potentials also constitute important contributions to $v_{\rm xc}$. In addition there is the potential $v_{\rm resp}$, which only enters $v_{\rm xc}$ but not $\varepsilon_{\rm xc}$ and represents ''response'' effects on $v_{\rm xc}^{\rm hole}$ and $v_{c,\rm kin}$. Details concerning the accurate configuration interaction (CI) calculations and the corresponding Kohn-Sham solutions are given in Sec. III. In Sec. IV a comprehensive discussion is given of $v_{\rm xc}$ and its components. Characteristic features in the shape of these potentials are related to the molecular electronic structure, in particular the behavior of Fermi and Coulomb correlation holes. Finally, $\varepsilon_{\rm xc}$ and its components ε_x and ε_c are considered in Sec. V. A comparison is made between the constructed $\varepsilon_{\rm xc}$, ε_x, and ε_c—keeping in mind their nonuniqueness—and the model exchange-correlation energy densities, such as the GGA models of Becke [22], and of Perdew and co-workers [15,23,24] for exchange and of Perdew and co-workers [15,23,24], and of Lee, Yang, and Parr [25] for Coulomb correlation. Also the corresponding GGA integrated exchange and correlation energies are compared to the ''exact'' quantities.

II. PARTITIONING OF THE KOHN-SHAM POTENTIAL $v_{\rm xc}$ AND THE RELATION BETWEEN $v_{\rm xc}$ AND THE EXCHANGE-CORRELATION ENERGY DENSITY $\varepsilon_{\rm xc}$

In this section we will present the definition of the KS functionals which can be constructed using *ab initio* wave functions. A central quantity of DFT is the electron density $\rho(\mathbf{r})$ which is represented in the KS theory as a sum over N occupied orbitals $\phi_i(\mathbf{r})$. Both the orbitals ϕ_i (which are functionals of the density) and the density ρ are used in the KS expression for the total electronic energy $E[\rho]$,

$$E[\rho]=T_s[\rho]+V[\rho]+W_H[\rho]+E_{\rm xc}[\rho]. \tag{2.1}$$

Here T_s is the kinetic energy of noninteracting particles ($\{\mathbf{x}_i\}=\{\mathbf{r}_i,s_i\}$, $\{\mathbf{r}_i\}$ are the space and s_i are the spin variables),

$$T_s[\rho]=-\tfrac{1}{2}\sum_{i=1}^{N}\int \phi_i^*(\mathbf{x})\nabla^2\phi_i(\mathbf{x})d\mathbf{x}. \tag{2.2}$$

V is the energy of electron-nuclear attraction, W_H is the Coulomb or Hartree energy of the electrostatic electron-electron repulsion, and $E_{\rm xc}$ is the (unknown) exchange-correlation energy functional. In order to subdivide $E_{\rm xc}$ into the exchange E_x and correlation E_c components, the determinant Ψ_s built from the KS orbitals ϕ_i is used as a reference wave function with the energy $E^{\rm KS}$,

$$E^{\rm KS}=\langle\Psi_s|\hat{H}|\Psi_s\rangle=T_s+V+W_H+E_x, \tag{2.3}$$

where $\hat{H}$ is the Hamiltonian of the system and E_x is the DFT definition for the exchange energy,

$$E_x=-\frac{1}{2}\sum_{i=1}^{N}\sum_{j=1}^{N}\int\frac{\phi_i^*(\mathbf{x}_1)\phi_j(\mathbf{x}_1)\phi_j^*(\mathbf{x}_2)\phi_i(\mathbf{x}_2)}{|\mathbf{r}_1-\mathbf{r}_2|}d\mathbf{x}_1d\mathbf{x}_2$$
$$=\frac{1}{2}\int\frac{\rho(\mathbf{x}_1)\rho_x(\mathbf{x}_2|\mathbf{x}_1)}{|\mathbf{r}_1-\mathbf{r}_2|}d\mathbf{x}_1d\mathbf{x}_2 \tag{2.4}$$

in which $\rho_x(\mathbf{x}_2|\mathbf{x}_1)$ is the exchange (Fermi) hole function. The correlation energy E_c in DFT is defined as the remainder when the exchange energy E_x defined above is subtracted from $E_{\rm xc}$, which implies that E_c is simply the difference between the exact energy E of Eq. (2.1) and $E^{\rm KS}$ of Eq. (2.3),

$$E_c=E_{\rm xc}-E_x=E-E^{\rm KS}. \tag{2.5}$$

The KS determinantal wave function thus plays the same role as the Hartree-Fock (HF) determinantal wave function does in the conventional definition, but now $E^{\rm KS}$ is defined in terms of the exact density ρ and corresponding KS orbitals ϕ_i, while $E^{\rm HF}$ is defined in terms of the HF density $\rho^{\rm HF}$ and the related HF orbitals.

We proceed with the definition of the exchange correlation energy density $\varepsilon_{\rm xc}$ [Eq. (1.1)] which allows its construction from *ab initio* first- and second-order density matrices. According to [9,10], $\varepsilon_{\rm xc}$ can be represented as the sum of kinetic $v_{c,\rm kin}$ and potential $v_{\rm xc}^{\rm hole}$ components as follows:

$$\varepsilon_{\rm xc}([\rho];\mathbf{x})=v_{c,\rm kin}([\rho];\mathbf{x})+\tfrac{1}{2}v_{\rm xc}^{\rm hole}([\rho];\mathbf{x}). \tag{2.6}$$

Here $v_{\rm xc}^{\rm hole}$ is the potential of the exchange-correlation hole. It cannot be obtained as a functional derivative but it can be expressed through the exchange-correlation hole function $\rho_{\rm xc}(\mathbf{x}_2|\mathbf{x}_1)$ defined in terms of the diagonal part of the second-order density matrix $\rho_2(\mathbf{x}_1,\mathbf{x}_2)$ or through the pair-correlation function $g^\lambda(\mathbf{x}_1,\mathbf{x}_2)$ with the electron interaction λ/r_{12} at full strength $\lambda=1$,

$$v_{\rm xc}^{\rm hole}(\mathbf{x}_1)=\int \frac{\rho_2(\mathbf{x}_1,\mathbf{x}_2)-\rho(\mathbf{x}_1)\rho(\mathbf{x}_2)}{|\mathbf{r}_1-\mathbf{r}_2|\rho(\mathbf{x}_1)}\,d\mathbf{x}_2$$
$$=\int \frac{\rho_{\rm xc}(\mathbf{x}_2|\mathbf{x}_1)}{|\mathbf{r}_1-\mathbf{r}_2|}\,d\mathbf{x}_2$$
$$=\int \frac{\rho(\mathbf{x}_2)[g^{\lambda=1}(\mathbf{x}_1,\mathbf{x}_2)-1]}{|\mathbf{r}_1-\mathbf{r}_2|}\,d\mathbf{x}_2. \quad (2.7)$$

The kinetic component $v_{c,\rm kin}$ [10,26] is the kinetic correlation energy density,

$$T_c=T-T_s=\int \rho(\mathbf{x})[v_{\rm kin}(\mathbf{x})-v_{s,\rm kin}(\mathbf{x})]d\mathbf{x}$$
$$=\int \rho(\mathbf{x})v_{c,\rm kin}(\mathbf{x})d\mathbf{x}. \quad (2.8)$$

In view of the recent comments by Huang and Umrigar [27] on the equality of expressions for $v_{c,\rm kin}$ (called τ_c in Ref. [27]) in terms of first or second derivatives of the one-electron density matrix we make the following observation. The quantities $v_{\rm kin}$ and $v_{s,\rm kin}$ are local potentials that are components of the effective local potential in the Schrödinger type of equation for the ''density orbital'' $\sqrt{\rho/N}$ [26,28]. $v_{\rm kin}$ results if the derivation is carried out [26] with the exact ground-state wave function Ψ_0 for the effective potential for the exact density, while $v_{s,\rm kin}$ results if the the derivation is carried out for the system of noninteracting Kohn-Sham electrons with wave function Ψ_s and of course the same density. It has been shown in Ref. [26] that $v_{\rm kin}$ and $v_{s,\rm kin}$ can be defined in terms of the conditional probability amplitudes [28] Φ of the total ground-state wave function

$$\Phi(\mathbf{x}_2,\ldots,\mathbf{x}_N|\mathbf{x}_1)=\frac{\Psi_0(\mathbf{x}_1,\ldots,\mathbf{x}_N)}{\sqrt{\rho(\mathbf{x}_1)/N}}, \quad (2.9)$$

$$v_{\rm kin}(\mathbf{x}_1)=\int [\Phi^*(\mathbf{x}_2,\ldots,\mathbf{x}_N|\mathbf{x}_1)\times(-\tfrac{1}{2}\nabla_1^2)\Phi(\mathbf{x}_2,\ldots,\mathbf{x}_N|\mathbf{x}_1)]d\mathbf{x}_2\cdots d\mathbf{x}_N \quad (2.10)$$

and similarly Φ_s of the KS determinant Ψ_s. For real wave functions it is easy to prove from the condition $\int\Phi^*(\mathbf{x}_2,\ldots,\mathbf{x}_N|\mathbf{x}_1')\Phi(\mathbf{x}_2,\ldots,\mathbf{x}_N|\mathbf{x}_1)d\mathbf{x}_2\cdots d\mathbf{x}_N=1$ for $\mathbf{x}_1'=\mathbf{x}_1$ that also the alternative expression

$$v_{\rm kin}(\mathbf{x}_1)=\int |\boldsymbol{\nabla}_1\Phi(\mathbf{x}_2,\ldots,\mathbf{x}_N|\mathbf{x}_1)|^2 d\mathbf{x}_2\cdots d\mathbf{x}_N \quad (2.11)$$

holds. This leads to two alternative expressions for $v_{\rm kin}$ in terms of the one-electron density matrix $\gamma(\mathbf{x}_1',\mathbf{x}_1)$ and the diagonal density $\rho(\mathbf{x}_1)=\gamma(\mathbf{x}_1,\mathbf{x}_1)$. The first [Eq. (26) in Ref. [26]] is

$$\rho(\mathbf{x}_1)v_{\rm kin}(\mathbf{x}_1)=-\frac{1}{2}\nabla_1^2\gamma(\mathbf{x}_1',\mathbf{x}_1)\Big|_{\mathbf{x}_1'=\mathbf{x}_1}-N\left(\frac{\rho(\mathbf{x}_1)}{N}\right)^{1/2}\times\left(-\frac{1}{2}\nabla_1^2\right)\left(\frac{\rho(\mathbf{x}_1)}{N}\right)^{1/2}, \quad (2.12)$$

which shows that $v_{\rm kin}$ is the energy density of the kinetic energy T minus the von Weiszäcker kinetic energy T_W, the latter being N times the kinetic energy of the density orbital $\sqrt{\rho/N}$. The second [Eq. (42) in Ref. [26]] is

$$\rho(\mathbf{x}_1)v_{\rm kin}(\mathbf{x}_1)=\frac{1}{2}\boldsymbol{\nabla}_1'\cdot\boldsymbol{\nabla}_1\gamma(\mathbf{x}_1',\mathbf{x}_1)\Big|_{\mathbf{x}_1'=\mathbf{x}_1}-\frac{|\boldsymbol{\nabla}_1\rho(\mathbf{x}_1)|^2}{8\rho(\mathbf{x}_1)}. \quad (2.13)$$

Similar expressions hold for $v_{s,\rm kin}$ in terms of the one-electron density matrix γ_s corresponding to the Kohn-Sham determinant Ψ_s. If we take the difference $v_{\rm kin}-v_{s,\rm kin}$, using either expressions (2.12) in both cases, or using expressions (2.13), the second term in these expressions cancels exactly since $\rho=\rho_s$. We may therefore write the kinetic correlation energy density either in terms of second derivatives or first derivatives of the one-electron density matrices,

$$\rho(\mathbf{x}_1)v_{c,\rm kin}(\mathbf{x}_1)=-\tfrac{1}{2}\nabla_1^2\gamma(\mathbf{x}_1',\mathbf{x}')\big|_{\mathbf{x}_1'=\mathbf{x}_1}+\tfrac{1}{2}\nabla_1^2\gamma_s(\mathbf{x}_1',\mathbf{x}_1)\big|_{\mathbf{x}_1'=\mathbf{x}_1}$$
$$=\tfrac{1}{2}\boldsymbol{\nabla}_1'\cdot\boldsymbol{\nabla}_1\gamma(\mathbf{x}_1',\mathbf{x}_1)\big|_{\mathbf{x}_1'=\mathbf{x}_1}-\tfrac{1}{2}\boldsymbol{\nabla}_1'\cdot\boldsymbol{\nabla}_1\gamma_s(\mathbf{x}_1',\mathbf{x}_1)\big|_{\mathbf{x}_1'=\mathbf{x}_1}. \quad (2.14)$$

In Ref. [26] and subsequent work [9,10] always the form with the first derivatives is used since the expansion in Gaussian basis functions leads to increased local inaccuracies for second derivatives [29].

We wish to stress that the well-known nonuniqueness of the kinetic energy density, alternative forms being obtained by carrying out a partial integration of the kinetic energy, does not pertain to $v_{c,\rm kin}$: $v_{c,\rm kin}$ is a unique function of position. Definition (2.6) of $\varepsilon_{\rm xc}$ is in fact in terms of potentials $v_{\rm xc}^{\rm hole}$ and $v_{c,\rm kin}$ that have a clear physical interpretation, and which are unique functions of position, being components of the exchange-correlation part $v_{\rm xc}$ of the KS potential (see below) which is known to be a unique function of position. In the DFT literature an alternative definition of $\varepsilon_{\rm xc}$ is often used, in which it is expressed via an integral over the coupling parameter γ [30,31],

$$\varepsilon_{\rm xc}(\mathbf{x}_1)=\frac{1}{2}\int\int_0^1 \frac{\rho(\mathbf{x}_2)[g^{\lambda}(\mathbf{x}_1,\mathbf{x}_2)-1]}{|\mathbf{r}_1-\mathbf{r}_2|}\,d\lambda\;d\mathbf{x}_2. \quad (2.15)$$

The nonuniqueness of the exchange-correlation energy density as a function of position is well known, as is the nonuniqueness of the kinetic energy density, but in this paper we choose definition (2.6) that is in terms of components of the KS potential that *are* unique functions of position. Expressions (2.7) and (2.14) allow us to construct $\varepsilon_{\rm xc}$ from *ab initio* first- and second-order density matrices, we do not need to know the dependence of g^{λ} on λ.

Using Eqs. (2.4) and (2.5) we can subdivide the exchange-correlation energy density into its exchange component,

$$\varepsilon_x(\mathbf{x}_1) = -\frac{1}{2\rho(\mathbf{x}_1)} \sum_{i=1}^{N} \sum_{j=1}^{N} \times \int \frac{\phi_i^*(\mathbf{x}_1)\phi_j(\mathbf{x}_1)\phi_j^*(\mathbf{x}_2)\phi_i(\mathbf{x}_2)}{|\mathbf{r}_1-\mathbf{r}_2|}\, d\mathbf{x}_2 = \frac{1}{2}\, v_x^{\text{hole}}(\mathbf{x}_1) \tag{2.16}$$

and its correlation component,

$$\varepsilon_c(\mathbf{x}_1) = \varepsilon_{\text{xc}}(\mathbf{x}_1) - \varepsilon_x(\mathbf{x}_1) = v_{c,\text{kin}}(\mathbf{x}_1) + \tfrac{1}{2} v_c^{\text{hole}}(\mathbf{x}_1), \tag{2.17}$$

where v_c^{hole} is the potential of the Coulomb correlation hole

$$v_c^{\text{hole}}(\mathbf{x}_1) = v_{\text{xc}}^{\text{hole}}(\mathbf{x}_1) - v_x^{\text{hole}}(\mathbf{x}_1) = \int \frac{\rho_c(\mathbf{x}_2|\mathbf{x}_1)}{|\mathbf{r}_1-\mathbf{r}_2|}\, d\mathbf{x}_2 . \tag{2.18}$$

Equation (2.6) for ε_{xc} also provides a partitioning of the exchange-correlation potential v_{xc}. Taking the functional derivative of $E_{\text{xc}}[\rho]$, Eqs. (1.1) and (1.2), leads to the following expression for v_{xc}:

$$v_{\text{xc}}([\rho];\mathbf{x}_1) = v_{\text{xc}}^{\text{hole}}([\rho];\mathbf{x}_1) + v_{c,\text{kin}}([\rho];\mathbf{x}_1) + v_{\text{resp}}([\rho];\mathbf{x}_1), \tag{2.19}$$

where $v_{\text{resp}}([\rho];\mathbf{r})$ is the ''response'' potential

$$v_{\text{resp}}([\rho];\mathbf{x}_1) = \frac{1}{2} \int \frac{\rho(\mathbf{x}_2)\rho(\mathbf{x}_3)}{|\mathbf{r}_2-\mathbf{r}_3|} \frac{\delta g^{\lambda=1}([\rho];\mathbf{x}_2,\mathbf{x}_3)}{\delta\rho(\mathbf{x}_1)}\, d\mathbf{x}_2 d\mathbf{x}_3 + \int \rho(\mathbf{x}_2) \frac{\delta v_{c,\text{kin}}([\rho];\mathbf{x}_2)}{\delta\rho(\mathbf{x}_1)}\, d\mathbf{x}_2 .$$

As was shown in [26,32], v_{resp} can be expressed also through the expectation values of the Hamiltonian of the $(N-1)$-electron system calculated with the conditional probability amplitudes Φ and Φ_s of Eq. (2.9).

In the next section a procedure for the numerical construction of v_{xc} and ε_{xc} and their components and the calculation of the KS energy characteristics will be outlined.

III. COMPUTATIONAL DETAILS

Since the scheme of v_{xc} and ε_{xc} construction from *ab initio* wave functions used in this paper has already been presented and discussed in [9,10], we will only give some specific details concerning the present calculations. The correlated reference densities and one- and two-electron density matrices have been obtained by means of Hartree-Fock and subsequent configuration interaction calculations using the ATMOL package [33]. We have calculated, in a basis of contracted Gaussian functions, the ground states of Li_2, N_2, and F_2 at the experimental equilibrium bond distances $R_e = 5.05$ a.u. for Li_2, $R_e = 2.074$ a.u. for N_2 and $R_e = 2.668$ a.u. for F_2. For Li a basis [34] with eight s- and four p-type functions has been used, which has been augmented with extra p and d polarization functions. For N and F the correlation-consistent polarized core-valence triple ζ added (CC-PCVTZ) basis sets [35] have been used. A more detailed discussion of the applied basis sets can be found in Ref. [36].

The multireference CI (MRCI) calculations have been carried out within the direct CI approach with 106 reference configurations for Li_2 and N_2 and 36 reference configurations for F_2. The reference configurations were selected within the internal space of eight lowest-energy Hartree-Fock molecular orbitals (MO) for Li_2 and ten orbitals for N_2 and F_2. All single and double excitations from each reference configuration to either internal or external subspaces have been included in the MRCI, which have also been augmented with the configurations obtained by single excitation from a reference configuration to the internal subspace with subsequent single excitation to the external subspace. The MRCI calculations performed at R_e recover 86% of the total Coulomb correlation energy for Li_2 and N_2, and 84% for F_2.

To construct v_{xc}, ε_{xc}, and their components, the first-order density matrix $\gamma(\mathbf{r}_1',\mathbf{r}_1)$, its diagonal part $\rho(\mathbf{r})$, and the diagonal part $\rho_2(\mathbf{r}_1,\mathbf{r}_2)$ of the second-order density matrix are calculated from the MRCI wave function by means of a Gaussian orbital density functional code [26,37] based on the ATMOL package.

The KS orbitals are constructed in an iterative procedure [6,8] in the same basis of MO's as has been used for the MRCI calculations. After 75–100 iterations the procedure has reached its saturation state and further iterations make changes only within a few millihartrees for the calculated KS orbital energies ε_i and the kinetic energy T_s. The accuracy of the resultant KS solution can be characterized by the values of the absolute integral error at mth iteration,

$$\Delta\rho = \int |\rho^m(\mathbf{r}) - \rho(\mathbf{r})|\, d\mathbf{r}, \tag{3.1}$$

with the values $\Delta\rho = 0.0035e$ for N_2, $\Delta\rho = 0.007e$ for F_2, and $\Delta\rho = 0.04e$ for Li_2 obtained after 100 iterations. The relatively large error for Li_2 appears, probably, because for this molecule with its diffuse electron density the region of density tails (where both the Gaussian basis set representation and the potential construction procedure are less adequate) plays a more important role.

IV. THE EXCHANGE-CORRELATION POTENTIAL AND ITS COMPONENTS

In Fig. 1 the molecular Kohn-Sham exchange-correlation potentials v_{xc} and their components $v_{\text{xc}}^{\text{hole}}$, $v_{c,\text{kin}}$, and v_{resp} constructed for Li_2, N_2, and F_2 at R_e(A-A) are plotted along the bond axis as functions of the distance z from the bond midpoint. The pictures thus represent the regions of σ bonds. In all cases both v_{xc} and $v_{\text{xc}}^{\text{hole}}$ are negative functions, with v_{xc} being consistently less attractive than the corresponding $v_{\text{xc}}^{\text{hole}}$. This can be understood from the fact that $v_{\text{xc}}^{\text{hole}}$ is the (negative) potential of a negative density, i.e., the exchange-correlation hole which represents the main correlation effect. According to Eq. (2.19), v_{xc} is formed by the addition of the usually repulsive contributions of $v_{c,\text{kin}}$ and v_{resp} to $v_{\text{xc}}^{\text{hole}}$.

The form of v_{xc} resembles that of $v_{\text{xc}}^{\text{hole}}$. In particular, both potentials have a deep well around the nucleus A, which corresponds to a strongly attractive exchange-correlation potential in the $1s$ core shell. Still, there exists a significant

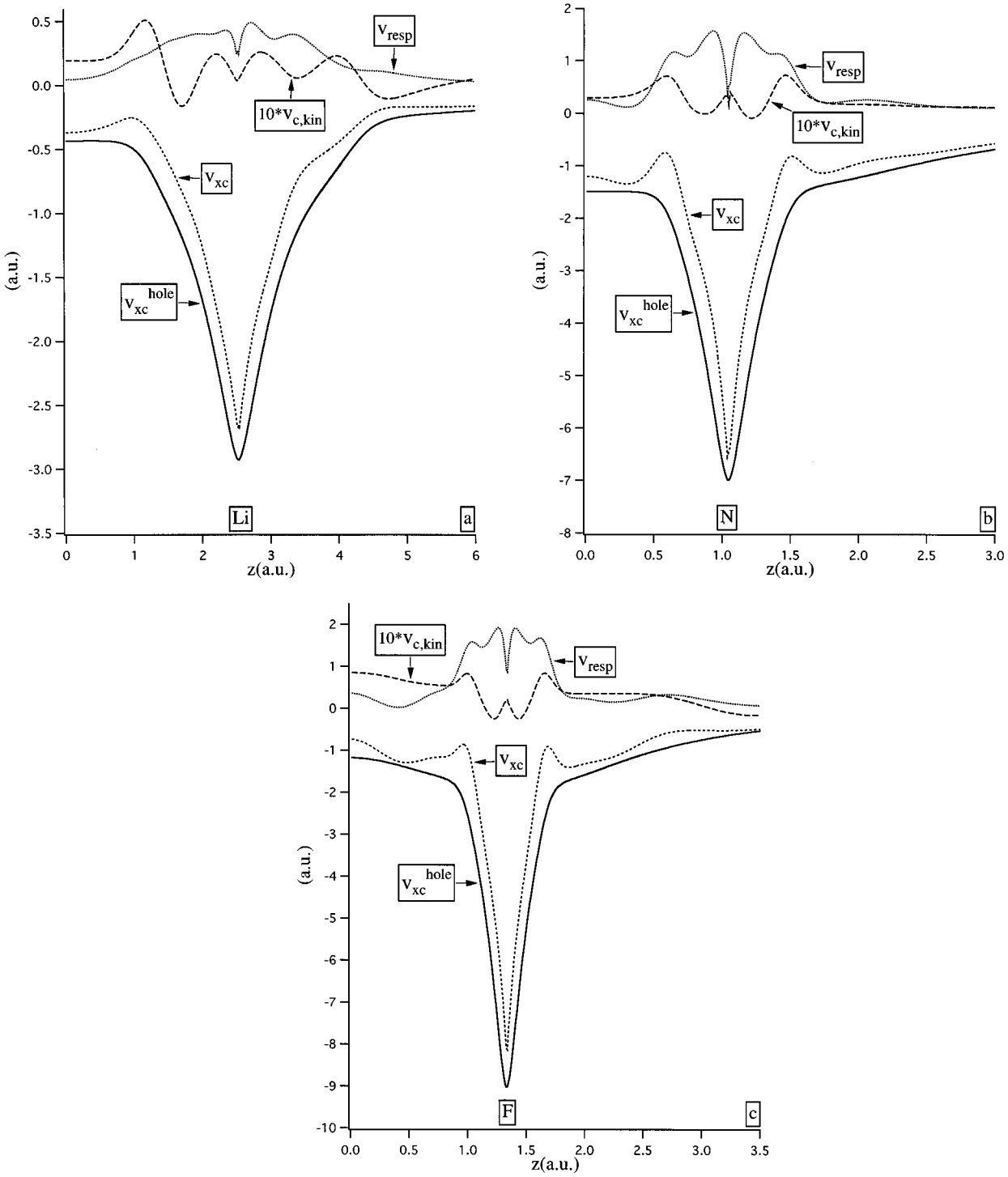

FIG. 1. The total exchange-correlation potential $v_{\rm xc}$ and its components, the potentials $v_{\rm xc}^{\rm hole}$, $v_{c,\rm kin}$, and $v_{\rm resp}$, along the bond axis at the equilibrium bond distance; z is the distance from the bond midpoint. (a) Li_2, (b) N_2, and (c) F_2.

difference between $v_{\rm xc}$ and $v_{\rm xc}^{\rm hole}$. The latter is a rather smooth potential, whose most visible feature is its different slope in the core and valence regions. It is interesting to note the somewhat different form of $v_{\rm xc}^{\rm hole}$ in the bonding and outer regions of Li_2 and N_2. While in the outer region (larger z values) $v_{\rm xc}^{\rm hole}$ smoothly approaches the Coulombic asymptotics $v_{\rm xc}^{\rm hole} \cong -1/r$, it forms a plateau in the bonding region (small z values). For N_2 this plateau is at significantly more negative energy than that for Li_2, which reflects the stronger exchange-correlation effects in the former case [see Figs. 1(a), 1(b)]. For F_2, on the other hand, $v_{\rm xc}^{\rm hole}$ in the bonding region does not clearly exhibit such a plateau, although it has a rather flat maximum at the bond midpoint [see Fig. 1(c)].

As will be shown in the next section, the dominant exchange component $v_x^{\rm hole}$ of $v_{\rm xc}^{\rm hole}$ which, according to Eq. (2.16), is twice the exchange energy density ε_x, displays a similar plateau for all three molecules considered. A possible interpretation of the plateau form of $v_{\rm xc}^{\rm hole}$ and ε_x around the

bond midpoint is that for the valence electrons of the σ bond this region is the interior region of the exchange (Fermi) hole which is delocalized symmetrically over both atoms of A_2 [38]. The hole has large depth around each nucleus, and the charge distribution of such a hole can be approximated effectively with a simple electrostatic model of two charges of $-0.5e$ which are placed along the bond axis at distances r and $-r$ from the bond midpoint. Furthermore, it is well known that the exchange hole of an electron pair bond is essentially static, i.e., it does not change shape when the reference position is changed around the bond midpoint [38]. We are thus led to consider the following very simple potential for small displacements z from the bond midpoint:

$$v_{\mathrm{mod}}(z) = -\frac{0.5}{r-z} - \frac{0.5}{r+z} \cong -\frac{1}{r}\left(1-\frac{z^2}{r^2}\right). \qquad (4.1)$$

Within this model the potential will only change in second order for small displacements ($z/r \ll 1$) from the bond midpoint, showing that our model potential is essentially flat around the bond midpoint. These simple electrostatic arguments indicate that the plateau of $v_{\mathrm{xc}}^{\mathrm{hole}}$ in the bonding region can be understood as a manifestation of the delocalized, static nature of the corresponding Fermi hole and the presence of the additional Coulomb hole, which at R_e is much weaker than the exchange hole, does not change this feature qualitatively for Li_2 and N_2.

Contrary to this, the addition of the Coulomb hole does change the form of $v_{\mathrm{xc}}^{\mathrm{hole}}$ in the bonding region of F_2 as was mentioned above. A possible interpretation is that in this case the addition of the Coulomb hole makes the total exchange-correlation hole substantially more localized on the atom where the reference electron is. A more pronounced effect of the Coulomb hole is expected when the bond is relatively long and weak (cf. H_2 at long distance in Ref. [38]), which is the case in F_2. As a result, the total hole starts to localize on the nucleus that is nearest when the reference position moves away from the bond midpoint, and the potential becomes Coulombic rather than flat. In the next section these qualitative arguments will be supported with the analysis of the constructed correlation energy density ε_c, which includes as a part the potential of the Coulomb correlation hole v_c^{hole}, Eq. (2.18).

In contrast to the rather structureless $v_{\mathrm{xc}}^{\mathrm{hole}}$, the total exchange-correlation potential v_{xc} displays a characteristic structure. The most visible features of v_{xc} are the local maxima (intershell peaks) between the core and valence regions of atom A. These peaks are clearly exhibited for N_2 at $z=0.6$ and 1.5 a.u., and for F_2 at $z=1.0$ and 1.6 a.u., while for Li_2 they are less pronounced. Beyond these peaks on the outer sides of the N and F atoms there are weak local minima, while for the lighter Li_2 molecule v_{xc} has a smooth monotonic form in this region. Another characteristic feature for Li_2 is that near the bond midpoint v_{xc} is almost parallel to $v_{\mathrm{xc}}^{\mathrm{hole}}$ as it forms a plateau. For N_2 and F_2 in contrast, v_{xc} displays, after passing through a local minimum, a bond midpoint ''peak'' [see Figs. 1(b) and 1(c)]. Since the $v_{c,\mathrm{kin}}$ and v_{resp} parts of v_{xc} are responsible for its observed structure, we will next analyze these contributions to v_{xc} in more detail.

The kinetic component $v_{c,\mathrm{kin}}$ of v_{xc} is defined by Eq. (2.11) in terms of the difference between the integrated squares of the gradients of the conditional amplitudes $|\boldsymbol{\nabla}_1\Phi|^2$ and $|\boldsymbol{\nabla}_1\Phi_s|^2$. In other words, $v_{c,\mathrm{kin}}$ represents the difference in sensitivity of the full exchange-correlation hole and the exchange-only (Fermi) hole in the distribution of the other electrons to displacement of the reference electron [10,26]. (Note that $v_{c,\mathrm{kin}}$ is enhanced by a factor of 10 in Fig. 1.)

The characteristic features of $v_{c,\mathrm{kin}}$ in the σ bond region are the $1s$-$2s$ intershell peaks, which occur for N_2 at about $z=0.5$ and 1.4 a.u. (for Li_2 at 1.1 and 4 a.u. and for F_2 at 1 and 1.6 a.u.) and which contribute to the above-mentioned corresponding peaks in v_{xc} at these positions. These peaks reflect the added effect of mobility of the Coulomb correlation hole when the reference electron crosses the intershell border, so that the corresponding change of the exchange-correlation hole is larger than that of the Fermi hole. They are analogous to the peaks observed and explained in Ref. [10] for the hydrides LiH, BH, and HF. In all cases the intershell peaks are clearly displayed as the largest ones on both sides of atom A. At smaller distances from the nucleus, in the core regions, there are also smaller peaks in $v_{c,\mathrm{kin}}$ which get considerably closer to the nucleus when going from Li_2 to N_2 and coalesce into a single peak at the nucleus for F_2. According to the interpretation given in [10], these peaks are related to the change in Coulomb hole from polarization to expansion shape in this region [38].

Another feature of $v_{c,\mathrm{kin}}$ is its definitely positive value in the bond midpoint region (in the case of F_2 even a peak). This also can be explained directly from the definition (2.11) in terms of the probability amplitudes (2.9) [26]. If the reference electron is displaced from a point $\mathbf{r}_1$ close to the bond midpoint towards a certain atom, the probability distribution of the second electron in this bond increases at the other atom due to the left-right Coulomb correlation. This causes a change in the exchange-correlation hole associated with Φ and produces positive values of the amplitude gradient $|\boldsymbol{\nabla}_1\Phi|^2$. In the corresponding KS case there is no analogous effect for $|\boldsymbol{\nabla}_1\Phi_s|^2$, since Φ_s describes a pure exchange hole which for an electron pair bond is independent of the position of the reference electron. Therefore the resulting $v_{c,\mathrm{kin}}$ is definitely positive in this region. As was established in [26] for H_2 and in [10] for the monohydrides XH, $X=$Li,B,F, the increasing left-right correlation provides an appreciable peak for the dissociating molecule, while for R_e the height of the ''peak'' (if any) is small. The present results for $v_{c,\mathrm{kin}}$ show a similar trend. The bond midpoint peak is displayed in $v_{c,\mathrm{kin}}$ for F_2, while for Li_2 and N_2 $v_{c,\mathrm{kin}}$ exhibits only a positive plateau in this region. This is in agreement with the observation made before that the σ bond in F_2 starts to exhibit behavior that is typical for stretched bonds. The Pauli closed-shell repulsion between the occupied p_π orbitals on the F atoms is indeed supposed to ''stretch'' the p_σ bond of F_2.

The response potentials v_{resp} plotted in Fig. 1 have been obtained by subtracting $v_{\mathrm{xc}}^{\mathrm{hole}}$ and $v_{c,\mathrm{kin}}$ from v_{xc}. The response potential is repulsive and has a characteristic steplike form with higher values for the core electrons, lower values for other electrons, and a steep descent from higher to lower values [10,32,39]. The typical height of the core step Δv_{resp}

of the constructed $v_{\rm resp}$ is in agreement with its rough estimate [40] for the case of the exchange-only potential v_x of the optimized potential model (OPM) [41–44],

$$\Delta v_{\rm resp} \approx 0.38\sqrt{\varepsilon_{\rm HOMO}-\varepsilon_i}, \tag{4.2}$$

where $\varepsilon_{\rm HOMO}$ denotes the energy of the highest occupied molecular orbital and ε_i is in this case the energy of the core orbital. The step pattern of $v_{\rm resp}$ is disturbed by cusps and wiggles near the nucleus, which might very well be caused by the incorrect Gaussian basis set representation of the density near the nucleus [29]. However, we have not further analyzed this point. Beyond the steep descent of $v_{\rm resp}$ on the outer side of the N and F atoms one can notice a small local maximum (for F_2, for instance, between $z=2.5$ and 3 a.u.), which is responsible for the corresponding feature of $v_{\rm xc}$.

An interesting feature of $v_{\rm resp}$ for N_2 and F_2 is that it displays a bond midpoint peak after passing through a minimum in the bonding region. The response potential for Li_2 lacks this peak and just goes through a rather shallow minimum at the bond midpoint. This peak in $v_{\rm resp}$, which for F_2 is higher than for N_2, is responsible for the same feature in $v_{\rm xc}$ for N_2 and F_2 (as opposed to the flat behavior of $v_{\rm xc}^{\rm hole}$). The presence of this repulsive feature in the potential for N_2 and F_2 correlates with the existence of a repulsive interaction (Pauli repulsion) between the occupied $2s$ subshells of the atoms N and F in N_2 and F_2. For the Li_2 molecule R_e(Li-Li) is large and the closed shells consist, apart from the single valence orbital, of the localized $1s$ core orbitals, which have very little overlap and therefore virtually no Pauli repulsion. This corresponds to the absence of a bond midpoint peak in $v_{\rm resp}$ for Li_2. We defer a discussion of the relation between Pauli repulsion and a bond midpoint peak in the response potential to a future paper, since this question is somewhat involved and has no bearing on the behavior of the energy densities ε_x and ε_c which we study in the next section, the response potential not being a component of these energy densities.

V. CONSTRUCTED AND MODEL (LDA AND GGA) EXCHANGE-CORRELATION ENERGY DENSITIES

The success of DFT is due to the existence of accurate exchange-correlation functionals $E_{\rm xc}[\rho]$ or rather exchange-correlation energy densities $\varepsilon_{\rm xc}[\rho](\mathbf{r})$, which integrate to reliable exchange-correlation energies. For many properties the LDA functionals are already quite accurate, for others (notably bond energies) the GGA functionals have brought considerable improvement. In order to study the local quality of the approximate energy densities we have constructed the exchange-correlation energy density per particle $\varepsilon_{\rm xc}$ numerically. In particular, we compare its exchange and correlation parts $\varepsilon_x=\frac{1}{2}\,v_x^{\rm hole}$ [Eq. (2.16)] and $\varepsilon_c=v_{c,\rm kin}+\frac{1}{2}\,v_c^{\rm hole}$ [Eq. (2.17)], with some of the currently used GGA functionals $\varepsilon_x^{\rm GGA}$ and $\varepsilon_c^{\rm GGA}$, which are explicit functions of the density ρ and its gradient $|\nabla\rho|$.

A. Correlation energy and energy density

Before discussing the Coulomb correlation energy density ε_c calculated as the difference between $\varepsilon_{\rm xc}$ and ε_x, or (equivalently) the sum of $\frac{1}{2}\,v_c^{\rm hole}$ and $v_{c,\rm kin}$, we first consider the following. While we expect that the KS orbitals and, hence, the KS exchange energy E_x obtained are of reasonable quality, the correlation energy E_c calculated with the restricted CI amounts to only about 85% of the total correlation energy, as was mentioned in Sec. III. The limitations on the CI calculation lead to E_c values which definitely underestimate the correlation of the core electrons as well as core-valence correlation and possibly to some extent also the interpair correlation of valence electrons.

In order to correct for this deficiency, we estimate the true DFT correlation energies from the conventional empirical correlation values $E_c^{\rm HF,emp}$ as they are traditionally defined in quantum chemistry. The $E_c^{\rm HF,emp}$ values have been obtained as the difference between the empirical total nonrelativistic electronic energy of a system $E^{\rm emp}$ estimated from spectroscopic data [45] and the Hartree-Fock electronic energy $E^{\rm HF}$,

$$E_c^{\rm HF,emp}=E^{\rm emp}-E^{\rm HF}. \tag{5.1}$$

Using the electronic energy $E^{\rm KS}$ of the KS system (2.3) calculated within the iterative procedure of Sec. III, we can obtain an estimate $E_c^{\rm emp}$ of the DFT correlation energy,

$$E_c^{\rm emp}=E^{\rm emp}-E^{\rm KS}=E_c^{\rm HF,emp}+(E^{\rm HF}-E^{\rm KS}), \tag{5.2}$$

which is presented in the row labeled ''KSemp'' of Table I. We feel that $E^{\rm GGA}$ should rather be compared to the empirical estimate of the true DFT correlation energy $E_c^{\rm emp}$. In fact, the GGA's are always judged by their performance for experimental (bond) energies.

For the same reason, we feel that $\varepsilon_c^{\rm GGA}$ should be compared to the scaled empirical energy density $\varepsilon_c^{\rm emp}$, defined by

$$\varepsilon_c^{\rm emp}(\mathbf{r})=\frac{E_c^{\rm emp}}{E_c}\,\varepsilon_c(\mathbf{r}), \tag{5.3}$$

which integrates to $E_c^{\rm emp}$. Meanwhile the form of $\varepsilon_c^{\rm GGA}$ will hardly change when the exact density is used in this functional instead of the present CI density.

In Fig. 2 we compare $\varepsilon_c^{\rm emp}$ with the LDA correlation functional $\varepsilon_c^{\rm LDA}$ [46] as well as with the GGA correlation functional of Perdew and co-workers (PW) $\varepsilon_c^{\rm PW}$ [15,23,24], and that of Lee, Yang, and Parr (LYP) $\varepsilon_c^{\rm LYP}$ [25], the latter being in the gradient-only form of Miehlich *et al.* [47]. We note that the $\varepsilon_c^{\rm LDA}$ curve differs considerably from the other curves. It is structureless and it is, in general, significantly lower than the other ones. This is due to the well-known difference in correlation between the homogeneous electron-gas model (which is represented by the LDA) and finite inhomogeneous atomic and molecular systems. All the structure in $\varepsilon_c^{\rm emp}$ arising from atomic shell effects and molecular bonding effects is absent from $\varepsilon_c^{\rm LDA}$. Moreover, it is known [48] that in the homogeneous electron gas the Coulomb correlation of electrons with like spins brings about the same contribution to E_c as that of the opposite-spin electrons. However, in finite systems correlation of like-spin electrons is substantially suppressed by their exchange, so that this brings only a small contribution to E_c. The local-density approximation therefore tends to overestimate correlation in finite closed-shell systems, and indeed it is obvious that $\varepsilon_c^{\rm LDA}$

TABLE I. Kohn-Sham, LDA, and GGA exchange and correlation energies (a.u.). The approximations for exchange and correlation are both indicated (e.g, B-PW: Becke for exchange, Perdew-Wang for correlation). The row labeled KS contains the ''exact'' correlation energy, i.e., the calculated CI energy minus the energy of the KS determinant, and the exchange energy evaluated with the KS orbitals. In the row KSemp the calculated CI energy has been replaced with the exact (spectroscopically determined) total energy.

		E_c	E_x	E_{xc}
Li_2	KS	-0.111	-3.565	-3.676
	KSemp	-0.128	-3.565	-3.693
		$E_c-E_c^{nd}=-0.119$	$E_x+E_c^{nd}=-3.574$	
	LDA	-0.330	-3.084	-3.414
	PW-PW	-0.137	-3.537	-3.674
	B-PW	-0.137	-3.555	-3.692
	B-LYP	-0.134	-3.555	-3.699
		-0.119	-3.574	
N_2	KS	-0.475	-13.114	-13.589
	KSemp	-0.552	-13.114	-13.666
		$E_c-E_c^{nd}=-0.476$	$E_x+E_c^{nd}=-13.190$	
	LDA	-0.942	-11.873	-12.815
	PW-PW	-0.490	-13.180	-13.670
	B-PW	-0.490	-13.208	-13.698
	B-LYP	-0.484	-13.208	-13.692
	KS	-0.475	-13.114	-13.589
	KSemp	-0.552	-13.114	-13.666
F_2	KS	-0.632	-19.935	-20.567
	KSemp	-0.755	-19.935	-20.690
		$E_c-E_c^{nd}=-0.676$	$E_x+E_c^{nd}=-20.014$	
	LDA	-1.296	-18.211	-19.507
	PW-PW	-0.669	-20.066	-20.735
	B-PW	-0.669	-20.101	-20.770
	B-LYP	-0.675	-20.101	-20.776

is consistently too negative. Because of this local overestimation of correlation, ε_c^{LDA}, when integrated against ρ, yields about 100% too negative correlation energies E_c^{LDA} (see Table I).

An important feature of the constructed ε_c^{emp} as well as of ε_c^{PW} and ε_c^{LYP} is their considerable amount of structure. All the functions have a well around the nucleus A, which represents correlation of the $1s$ core electrons. The average depth of the well does not increase with atomic number of A. This reflects the fact that for neutral systems the contribution to E_c from the $1s$ electron pair does not depend much on the atomic number of the corresponding atom. In this respect, correlation of the $1s$ electrons differs from their exchange, which almost completely reduces to the self-interaction of the $1s$ electron. As can be seen from Fig. 3, the depth of the well of the exchange energy density ε_x around the nucleus does increase with increasing atomic number due to the increasingly contracted nature of the $1s$, leading to stronger self-interaction.

The wells in ε_c^{emp}, ε_c^{PW}, and ε_c^{LYP} are terminated by peaks in the K-L intershell region, at distances of about ± 1.4 a.u. (Li_2), ± 0.4 a.u. (N_2), and ± 0.3 a.u. (F_2) from the nuclei. Comparison with Fig. 1 shows that in the case of the constructed ε_c^{emp} these peaks are determined, primarily, by the corresponding peaks in the kinetic part $v_{c,kin}$. Beyond the intershell peaks there are distinct wells in ε_c^{emp} for N_2 and F_2, which in the case of F_2 are even lower than the well at the position of the nucleus. Going next to the bond midpoint, one notes a striking difference between the three molecules. The ε_c^{emp} of Li_2 becomes perfectly flat after the inner $1s$-$2s$ intershell peak, but for N_2 there is a clear bond midpoint peak, which for F_2 becomes relatively high and even reaches positive values [see Fig. 4(c)]. Since v_c^{hole}, the potential energy part of ε_c^{emp}, is an everywhere negative potential, this indicates that features of both the kinetic part $v_{c,kin}$ and the potential energy part v_c^{hole} contribute to the bond midpoint peak in ε_c^{emp}. The form of ε_c^{emp} in the bonding region resembles that for the H_2 molecule [38], where a peak around the bond midpoint arises from a peak in the (still negative) ν_c^{hole} and a positive peak in $\nu_{c,kin}$, originating from left-right correlation. The Coulomb hole representing the left-right correlation is negative around the nucleus nearest to the reference electron and it is positive at the other nucleus. When the reference electron crosses the bond midpoint, the Coulomb hole ''jumps,'' [26] changing its sign around the nuclei, which leads to a bond midpoint peak in $\nu_{c,kin}$ and hence in ε_c^{emp}. In the case of F_2 this type of left-right correlation will occur for the electrons of the relatively weak single σ bond. For N_2 the well in ε_c^{emp} beyond the outer peak is significantly deeper than that in the bonding region and the bond midpoint peak is relatively small. In this case, the bond midpoint peak of ε_c^{emp} reflects entirely the maximum in the correlation hole potential ν_c^{hole}, since $\nu_{c,kin}$ for N_2 lacks a corresponding peak in this region.

Keeping in mind that only tentative conclusions can be drawn from comparison of the various energy densities, in view of their nonuniqueness, we can make the following observations. It is interesting to note that the shape of the GGA functionals ε_c^{PW} and ε_c^{LYP} resembles that of ε_c^{emp} much better than ε_c^{LDA} does. Still, there is an appreciable difference between the two GGA functionals. In the case of Li_2, the outer intershell peak in ε_c^{LYP} is much larger than the peak in the bonding region, while both peaks in ε_c^{PW} are somewhat more shallow. On the other hand, for N_2 and F_2 it is ε_c^{PW} that has more pronounced intershell peaks and also wells beyond the peaks, as well as a deep well at the nucleus, while ε_c^{LYP} is a rather more shallow function for these molecules. Taking into account also the relatively deep well at the nucleus, ε_c^{PW} has a certain shape resemblance with the constructed ε_c^{emp}, although this similarity is by no means quantitative. Especially in the the bonding region of N_2 and F_2 all the model functionals are very different from the constructed ε_c^{emp}. Near the bond midpoint ε_c^{PW} consistently reduces to the flat and much too negative ε_c^{LDA}. This is a characteristic feature of all functionals that, like the PW one, are based on the electron-gas model and include only gradient-dependent corrections to ε_c^{LDA}. In the limit of a small density gradient $\nabla\rho\rightarrow 0$, as occurs near the bond midpoint, such functionals turn into ε_c^{LDA} by construction. In its turn, ε_c^{LYP} reduces to the Wigner-type formula for small gradients. This functional is also derived from the homogeneous electron-gas model but with the parameters fitted for the He atom. Because of this, ε_c^{LYP} does not reduce to ε_c^{LDA} near the bond midpoint

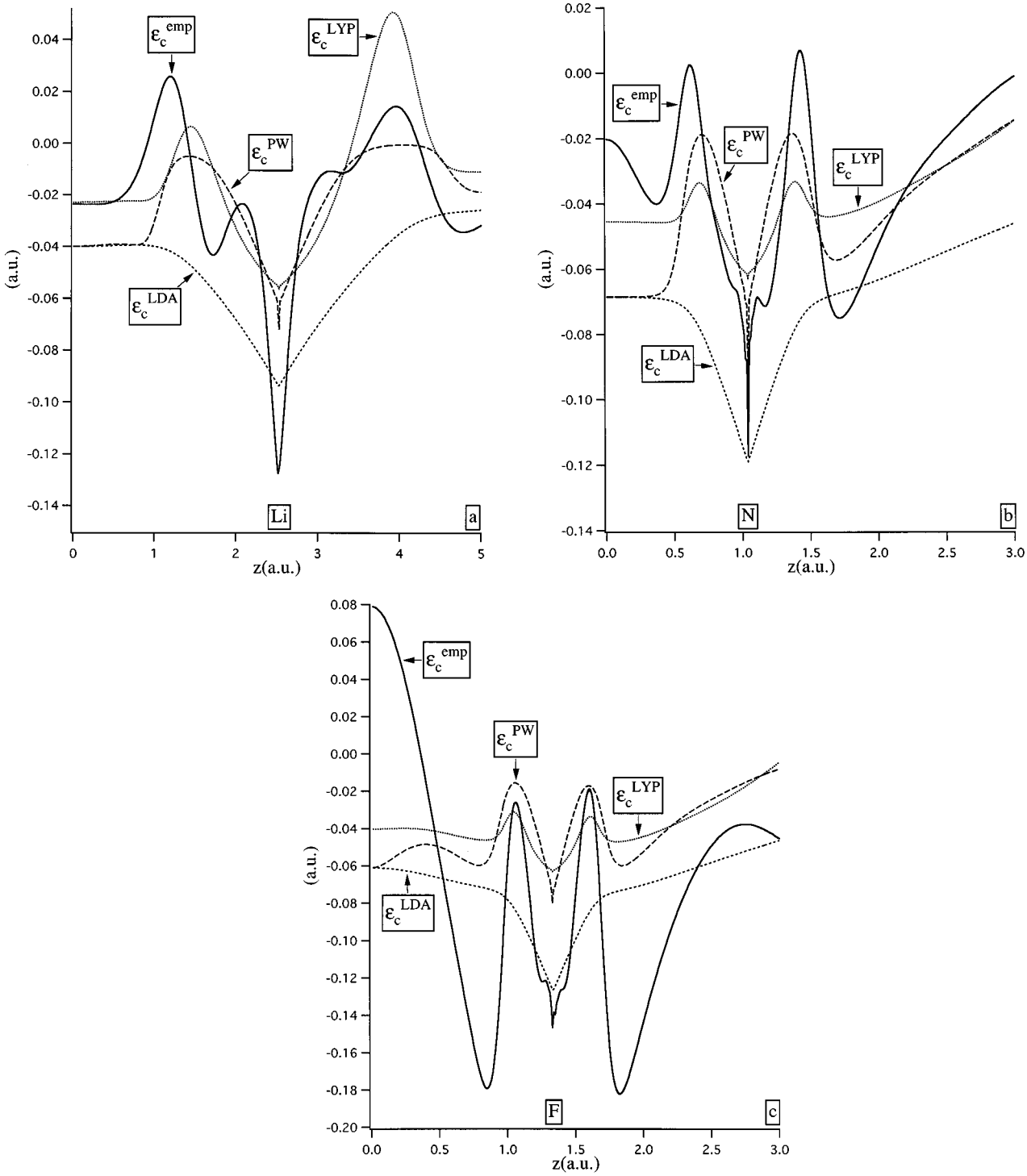

FIG. 2. The constructed empirical correlation energy density $\varepsilon_c^{\text{emp}}$ ($\varepsilon_c^{\text{CI}}$ scaled so as to integrate to the empirical correlation energy) and the corresponding LDA functional $\varepsilon_c^{\text{LDA}}$ and the GGA functionals of Perdew and co-workers $\varepsilon_c^{\text{PW}}$ and Lee, Yang, and Parr, $\varepsilon_c^{\text{LYP}}$, along the bond axis at the equilibrium bond distance; z is the distance from the bond midpoint. (a) Li_2, (b) N_2, and (c) F_2.

and it is closer to $\varepsilon_c^{\text{emp}}$ than $\varepsilon_c^{\text{PW}}$ is in this region. Still, $\varepsilon_c^{\text{LYP}}$ always has a flat form and it does not exhibit the bond midpoint peak for N_2 and F_2 which is such a distinct feature, related to left-right correlation, of $\varepsilon_c^{\text{emp}}$.

The first column in Table I presents the integrated correlation energies E_c (rows labeled KS and KSemp), E_c^{LDA} (row LDA), E_c^{PW} (rows PW-PW and B-PW) and E_c^{LYP} (row B-LYP). Comparing the E_c^{GGA} to E_c^{emp}, since the GGA functionals should give the full correlation energy, we conclude that the E_c^{GGA} amount to only 84–89 % of the true correlation energy. The discrepancies between E_c^{GGA} and E_c^{emp} are significant: for N_2 the largest difference between E_c^{GGA} and E_c^{emp} is 0.068 hartree for E_c^{LYP} and for F_2 the largest difference is 0.086 hartree for E_c^{PW}.

We have argued elsewhere [36] that the E_c^{GGA} correlation energies are too small compared to E_c^{emp} since they do not

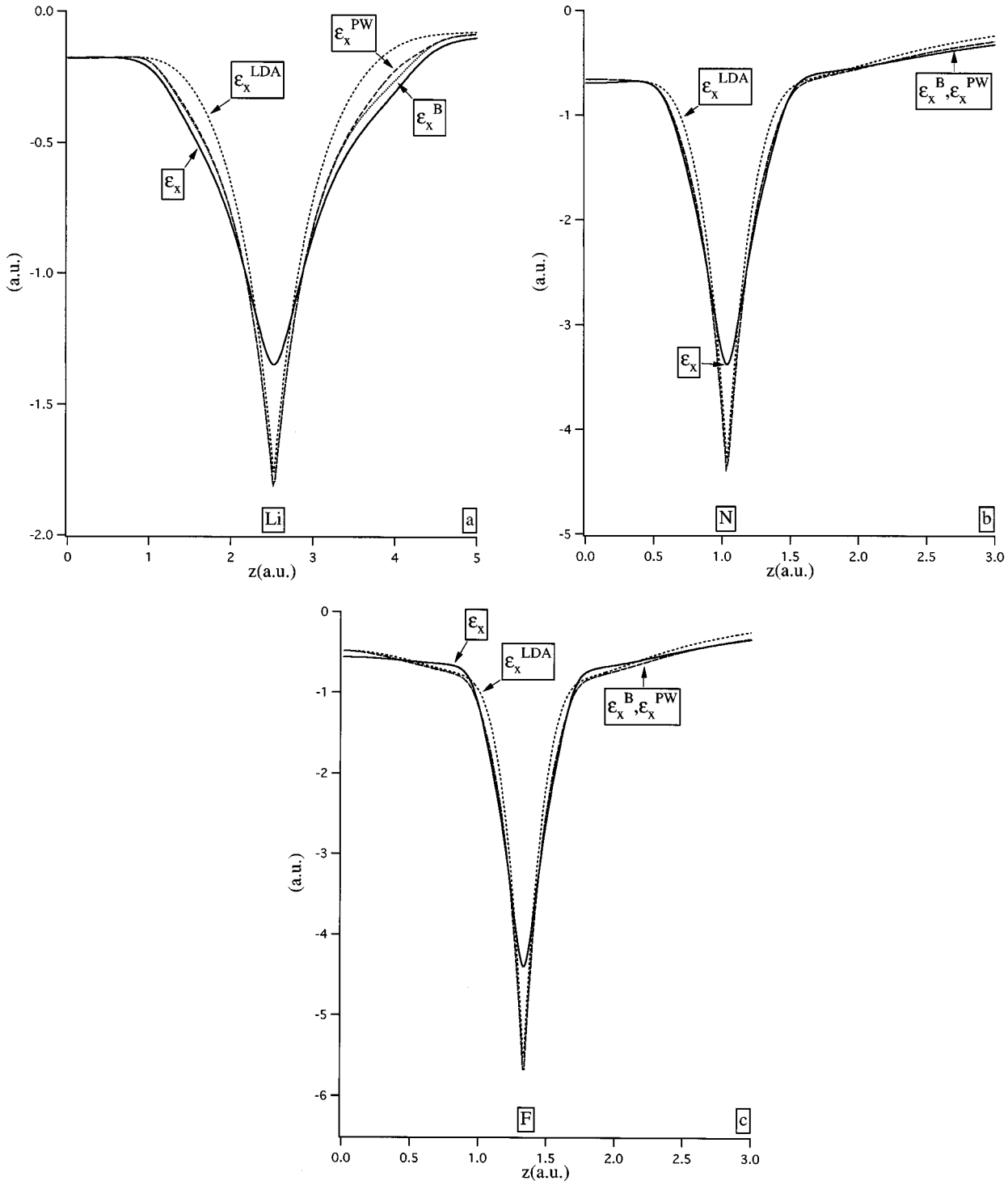

FIG. 3. The constructed exchange energy density ε_x and the corresponding LDA functional $\varepsilon_x^{\mathrm{LDA}}$ and the GGA functionals of Becke, ε_x^B, and Perdew and co-workers, $\varepsilon_x^{\mathrm{PW}}$, along the bond axis at the equilibrium bond distance, z is the distance from the bond midpoint. (a) Li_2, (b) N_2, and (c) F_2.

incorporate all of the electron correlation. The effect of the left-right correlation discussed above, which deepens the Coulomb hole around the reference electron, may be missing. Indeed, the LDA and GGA correlation functionals have been developed from the homogeneous or inhomogeneous electron gas, which (at least for the densities ρ typical for atomic and molecular systems) does not contain the phenomenon of left-right correlation. In the prototype case of dominating left-right correlation, nearly dissociated H_2, it has been shown [9] that indeed $\varepsilon_c^{\mathrm{GGA}}$ completely fails to describe ε_c, while also E_c^{PW} at R(H-H)=5 a.u. covers less than 20% of E_c [49]. We have noticed above the lack of the bond midpoint peak, related to left-right correlation, in the $\varepsilon_c^{\mathrm{GGA}}$ of N_2 and F_2. Even though the left-right correlation, or more generally the so-called nondynamical or near-degeneracy correlation is probably missing from the GGA's for correlation, the rest of the correlation effect, the so-called dynami-

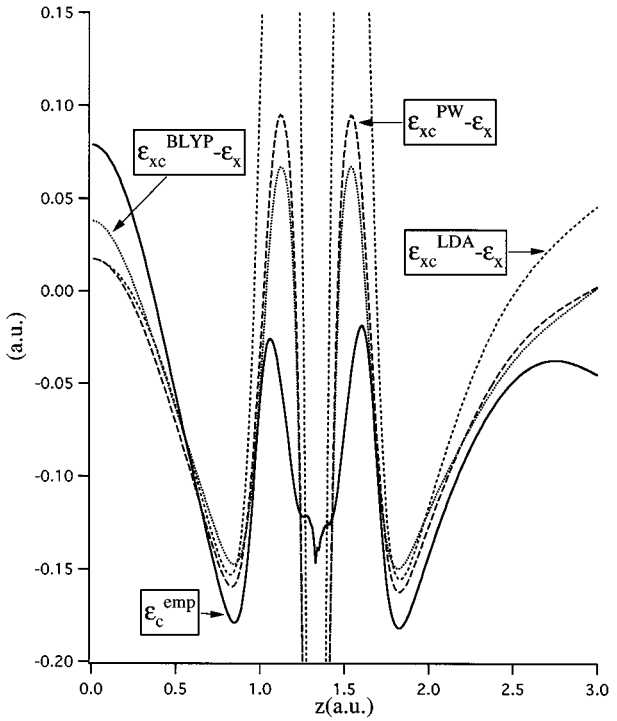

FIG. 4. Comparison between the constructed empirical correlation energy density $\varepsilon_c^{\rm emp}$ and the GGA correlation energy densities to which $\varepsilon_x^{\rm GGA}(\mathbf{r})-\varepsilon_x(\mathbf{r})$ is added as a possible representation of the contribution of nondynamical correlation.

cal correlation, is hopefully described by the electron-gas based correlation functionals.

The energy of nondynamical correlation $E_c^{\rm nd}$ can be estimated assuming that the simple CI wave functions constructed in Ref. [34], which provide the proper dissociation limit (PDL) for the dimers A_2, take into account the effect of nondynamical correlation and neglect dynamical correlation. With this assumption the energy $E_c^{\rm nd}$ can be estimated as the difference between the electronic energies of the PDL and HF functions, $E_c^{\rm nd}=E^{\rm PDL}-E^{\rm HF}$. This yields $E_c^{\rm nd}$ values of -0.009, -0.076, and -0.079 hartree for Li_2, N_2, and F_2, respectively. Thus the energy effect of nondynamical correlation at $R_e(A\text{-}A)$ is small for Li_2, while it is appreciable for N_2 and F_2. In Table I we present the energy of dynamical correlation E_c^d estimated as the difference $E_c^d=E_c^{\rm emp}-E_c^{\rm nd}$. The energies E_c^d appear to be close to the GGA correlation energies

$$E_c^{\rm GGA}\cong E_c^d. \tag{5.4}$$

Thus we arrive at the conclusion [36] that the GGA correlation functionals $E_c^{\rm GGA}[\rho]$ ($E_c^{\rm PW}$ or $E_c^{\rm LYP}$) effectively model the dynamical correlation of electrons only. We will return to the implications of this finding for the local differences between the energy densities $\varepsilon_c^{\rm GGA}$ and ε_c later, but first turn to ε_x.

B. Exchange energy and energy density

In Fig. 3 the exchange energy densities calculated from the KS orbitals ϕ_i via Eq. (2.16) at $R_e(A\text{-}A)$ are plotted along the bond axis as functions of the distance z from the bond midpoint. A comparison is made between ε_x and the exchange functional $\varepsilon_x^{\rm LDA}$ of the local-density approximation as well as with the GGA exchange functionals of Becke (B), ε_x^B [22], and of Perdew and co-workers, $\varepsilon_x^{\rm PW}$ [15,23,24]. In both GGA functionals $\varepsilon_x^{\rm LDA}$ is augmented with a correction factor, which is a function of the dimensionless gradient-dependent argument $|\nabla\rho|/\rho^{4/3}$. In connection with the nonuniqueness of the energy density, we note that the LDA and Becke functional were indeed designed to approximate the same exchange hole that we use in our definition of the exchange energy density $\varepsilon_x=(1/2)\nu_x^{\rm hole}$, Eq. (2.16). This does not hold for $\varepsilon_x^{\rm PW}$, but this energy density was characterized by its authors as being nearly identical to ε_x^B. We therefore feel that in this case ε_x and the $\varepsilon_x^{\rm GGA}$ are more strictly comparable. The second column in Table I presents the corresponding exchange energies E_x (rows labeled KS and KSemp), $E_x^{\rm LDA}$ (row LDA), $E_c^{\rm PW}$ (row PW-PW) and E_x^B (row B-PW and B-LYP).

Being the dominant component of the potential $\nu_{\rm xc}^{\rm hole}$ analyzed in Sec. IV, ε_x has the same general features, namely, a deep well around the nucleus, the asymptotical Coulombic-like behavior at larger z, and a plateau in the bonding region (see Fig. 3). The plateau is observed for all three molecules considered and its presence has been interpreted in the preceding section as a manifestation of a static delocalized Fermi hole for electrons of the σ bond of A_2. A general trend for $\varepsilon_x^{\rm LDA}$ is that it overestimates exchange near the nuclei, while it clearly underestimates exchange at distances r_A of a few tenths of an a.u. from the nucleus. It also slightly underestimates exchange at larger r_A, both in the outer region and around the bond midpoint (for Li_2 $\varepsilon_x^{\rm LDA}$ nearly coincides with ε_x around the bond midpoint). The LDA underestimation of exchange at intermediate r_A, where the density is still appreciable and the volume of the region is fairly large, overcompensates its considerable overestimation close to the nucleus, where the density is high but the volume very small. As a consequence the LDA exchange energies E_x are considerably smaller (less negative) than the KS energies E_x (see Table I).

The GGA gradient corrections to $\varepsilon_x^{\rm LDA}$ are everywhere negative functions that shift the LDA curve downwards and bring $\varepsilon_x^{\rm GGA}$ closer to ε_x in the important region at intermediate r_A. The gradient approximations, however, worsen the situation in the narrow region around the nucleus, and have little effect in the bonding region. The functional $\varepsilon_x^{\rm PW}$ is indeed, as noted by its authors, hardly distinguishable from ε_x^B. Note that contrary to $\varepsilon_x^{\rm PW}$, ε_x^B has the correct Coulombic asymptotics $-1/(2r)$ at large z, but one can hardly see this difference for the distances presented. Both ε_x^B and $\varepsilon_x^{\rm PW}$ approach ε_x more closely at larger z than $\varepsilon_x^{\rm LDA}$ does. In the bond midpoint region ε_x^B and $\varepsilon_x^{\rm PW}$ are very close to $\varepsilon_x^{\rm LDA}$. This is understandable, because for a homoatomic molecule the bond midpoint is at the same time a saddle point of the density ρ, where $|\nabla\rho|=0$. Due to this, the GGA argument $|\nabla\rho|/\rho^{4/3}$ is small in the bond midpoint region, providing a small GGA gradient correction. In particular, for F_2 there is a notable difference between the model and exact ε_x curves in the bonding region, both the LDA and GGA ε_x curves devi-

ating from the flat plateaulike behavior of ε_x. We will return to the meaning of this difference later.

The gradient corrections bring in the present series of molecules the GGA exchange energies E_x^{GGA} much closer to E_x as compared to E_x^{LDA}, as they are known to do (actually designed to do) in the case of atoms. In particular, for Li_2 the negative difference between $\varepsilon_x^{\mathrm{GGA}}$ and ε_x in the region near the nucleus [see Fig. 5(a)] appears to be almost perfectly compensated with their positive difference at larger r_A, so that E_x^B is only 10 millihartrees off the E_x value. However, for N_2 and F_2 the gradient corrections seem to overperform and the negative differences between E_x^{GGA} and E_x are considerably larger than the errors in the GGA correlation energies: the largest difference is between E_x^B and E_x and amounts to -0.094 hartree for N_2 and to -0.166 hartree for F_2. Although these errors are fairly small as a percentage of the total exchange energy, they are an appreciable fraction (in the order of 25%) of the total correlation energy (see Table I and the discussion below). In spite of the impression given by Fig. 3 of close agreement between the GGA and KS exchange energy densities over large regions of space, these results show that the difference between the LDA and GGA exchange energy densities and the KS exchange energy density is significant. Furthermore, the local differences $\varepsilon_x^{\mathrm{GGA}}(\mathbf{r})-\varepsilon_x(\mathbf{r})$ are large compared to, for instance, the PW correlation energy density $\varepsilon_c^{\mathrm{PW}}(\mathbf{r})$. Apart from the region around the nucleus, there are also large differences at the intershell peaks and in the bonding region (note that the peak around the bond midpoint corresponds to the deviation of the model exchange energy densities from the plateaulike behavior of ε_x noted above). It is in fact due to cancellation of positive and negative contributions that $\varepsilon_x^{\mathrm{GGA}}(\mathbf{r})-\varepsilon_x(\mathbf{r})$ integrates to only about 25% of the total correlation energy.

The LDA and the GGA (at least Becke, but PW is close) exchange energy densities try to model the KS exchange energy density by the potential of the exchange hole of the homogeneous or inhomogeneous electron gas. Maybe the errors noted above could have been expected if we recall that the KS exchange energy density is determined by the potential of a *delocalized* Fermi hole, while in the electron gas the hole is centered at the reference electron. It has been suggested [50–52] that in molecules the LDA exchange functional ($X\alpha$), since it mimics a localized hole, effectively describes the combined effect of exchange and nondynamical (left-right) correlation. As discussed earlier, this combined effect introduces partial localization of the exchange-correlation hole at the atom where the reference electron is residing, and the same localization is effectively provided by an exchange functional that employs the local density and density gradient. It is interesting to investigate (cf. also Ref. [36]) to what extent this qualitative notion is corroborated by the integrated GGA exchange energies (the LDA approximation to the exchange functional is too crude, the LDA exchange energies are too small rather than too large). We present in Table I the sum $(E_x+E_c^{\mathrm{nd}})$ of the KS exchange energy E_x and the energy of nondynamical correlation E_c^{nd} estimated above. It appears that the GGA ''exchange'' energies are actually much closer to the sum of exchange and nondynamical correlation energies

$$E_x^{\mathrm{GGA}} \cong E_x + E_c^{\mathrm{nd}}. \tag{5.5}$$

In particular, E_x^{GGA} (especially, the PW one) for N_2 are close to the sum $(E_x+E_c^{\mathrm{nd}})$. For F_2 the energies E_x^{GGA} are still too negative, but they are clearly much closer to $(E_x+E_c^{\mathrm{nd}})$ than to the bare exchange energy E_x. For Li_2 we have already shown that the effect of nondynamical correlation is small at R_e(Li-Li) and Eq. (5.5) therefore effectively reduces to $E_x^{\mathrm{GGA}} \cong E_x$.

C. The energy density of nondynamical correlation

We have arrived at the conclusion that on one hand E_c^{GGA} does not include nondynamical correlation, while on the other hand E_x^{GGA} does include this part of the correlation energy. One wonders if this point of view is not only substantiated by the values for the integrated quantities, but can also be traced in the shape of the energy densities as functions of position. Since the exchange GGA functionals have not been constructed with the purpose to contain features corresponding to nondynamical correlation, and since our choice of $\varepsilon_c(\mathbf{r})$ is not precisely the energy density the models strive to mimic, we cannot push this analysis too far. We just comment on the possibility, suggested by the above analysis, that local ''errors'' in $\varepsilon_x^{\mathrm{GGA}}(\mathbf{r})$ and $\varepsilon_c^{\mathrm{GGA}}(\mathbf{r})$ reflect unintended presence or neglect, respectively, of nondynamical correlation and cancel each other. This would mean that $\varepsilon_x^{\mathrm{GGA}}(\mathbf{r})-\varepsilon_x(\mathbf{r})$, representing nondynamical correlation, has to be added to $\varepsilon_c^{\mathrm{GGA}}(\mathbf{r})$, yielding $\varepsilon_{\mathrm{xc}}^{\mathrm{GGA}}(\mathbf{r})-\varepsilon_x(\mathbf{r})$, in order to make a meaningful comparison to the KS $\varepsilon_c^{\mathrm{emp}}(\mathbf{r})$ possible. Of course some variation is obtained in this comparison depending on which GGA is used, but we do obtain very significant qualitative improvement when comparing $\varepsilon_{\mathrm{xc}}^{\mathrm{GGA}}(\mathbf{r})-\varepsilon_x(\mathbf{r})$ rather than $\varepsilon_c^{\mathrm{GGA}}(\mathbf{r})$ to $\varepsilon_c^{\mathrm{emp}}(\mathbf{r})$. This is strikingly demonstrated for F_2 in Fig. 4, in which we compare $\varepsilon_c^{\mathrm{emp}}(\mathbf{r})$ to the energy densities obtained by adding $\varepsilon_x^{\mathrm{LDA}}(\mathbf{r})-\varepsilon_x(\mathbf{r})$ to $\varepsilon_c^{\mathrm{LDA}}(\mathbf{r})$, $\varepsilon_x^B(\mathbf{r})-\varepsilon_x(\mathbf{r})$ to $\varepsilon_c^{\mathrm{LYP}}(\mathbf{r})$, and finally $\varepsilon_x^{\mathrm{PW}}(\mathbf{r})-\varepsilon_x(\mathbf{r})$ to $\varepsilon_c^{\mathrm{PW}}(\mathbf{r})$. Most notably, the peak at the bond midpoint, which we identified as a left-right correlation effect in ε_c, is built in by the model exchange functionals. It would arise both from the LDA and GGA exchange functionals, cf. the difference between the model $\varepsilon_x^{\mathrm{LDA}}(\mathbf{r})$, $\varepsilon_x^{\mathrm{GGA}}(\mathbf{r})$, and the plateaulike behavior of $\varepsilon_x(\mathbf{r})$ in Fig. 3(c). The correspondence is also much improved in the wells, but addition of $\varepsilon_x^{\mathrm{GGA}}(\mathbf{r})-\varepsilon_x(\mathbf{r})$ and especially $\varepsilon_x^{\mathrm{LDA}}(\mathbf{r})-\varepsilon_x(\mathbf{r})$ leads to exaggeration at the intershell peaks. The well around the nucleus is of course strongly overestimated, the very deep well at the nucleus being a deficiency of the LDA and GGA exchange functionals that is not related to nondynamical correlation. Qualitatively similar improvement is obtained for the other molecules, although not so spectacular as for F_2. At a qualitative level, however, the local behavior of the $\varepsilon_c(\mathbf{r})$ and $\varepsilon_x(\mathbf{r})$ curves supports our contention that nondynamical correlation is lacking in the model $\varepsilon_c(\mathbf{r})$ curves, but is incorporated in the model $\varepsilon_x(\mathbf{r})$ curves.

We conclude by considering the total exchange-correlation energy density. Since the Coulomb correlation effect is small compared to the exchange, $\varepsilon_{\mathrm{xc}}(\mathbf{r})$ is practically indistinguishable from its exchange component $\varepsilon_x(\mathbf{r})$ displayed in Fig. 3. As a matter of fact, we have just ob-

served that locally differences $\varepsilon_x^{\mathrm{GGA}}(\mathbf{r})-\varepsilon_x(\mathbf{r})$ cancel to a large extent against differences $\varepsilon_c^{\mathrm{GGA}}(\mathbf{r})-\varepsilon_c^{\mathrm{emp}}(\mathbf{r})$, so agreement of $\varepsilon_{\mathrm{xc}}^{\mathrm{LDA}}$ and especially $\varepsilon_{\mathrm{xc}}^{\mathrm{GGA}}$ with $\varepsilon_{\mathrm{xc}}^{\mathrm{emp}}$ will be better than in the exchange-only case. For F_2 notably the clear difference in slope of both the $\varepsilon_x^{\mathrm{LDA}}$ and the $\varepsilon_x^{\mathrm{GGA}}$'s compared to ε_x is no longer present in the $\varepsilon_{\mathrm{xc}}$ curves. The most conspicuous discrepancy in $\varepsilon_x^{\mathrm{GGA}}$, the much too negative behavior at the nucleus, of course survives in $\varepsilon_{\mathrm{xc}}^{\mathrm{GGA}}$. At larger distances from the nucleus $\varepsilon_{\mathrm{xc}}^{\mathrm{GGA}}$ follows $\varepsilon_{\mathrm{xc}}$ rather closely indeed, but not perfectly. The local differences have opposite signs in different regions, thus compensating each other to some extent in the resulting GGA exchange-correlation energies. In particular, for Li_2 the B-PW value $E_{\mathrm{xc}}^{\mathrm{BPW}}=-3.692$ hartrees practically coincides with the corresponding KS value $E_x+E_c^{\mathrm{emp}}=-3.693$ hartrees and the PW-PW and B-LYP values are also close to $E_x+E_c^{\mathrm{emp}}$. Similarly, for N_2 the PW-PW value $E_{\mathrm{xc}}^{\mathrm{PW}}=-13.67$ hartrees is very close to the KS value $E_x+E_c^{\mathrm{emp}}=-13.666$ hartrees and the B-PW and B-LYP values are not very far from $E_x+E_c^{\mathrm{emp}}$. For F_2 there is also considerable compensation of the local errors of opposite signs, but a somewhat larger difference between the KS and GGA values for E_{xc} remains (see Table I).

VI. CONCLUSIONS

In this paper the molecular Kohn-Sham exchange-correlation potentials v_{xc} and the energy densities $\varepsilon_{\mathrm{xc}}$ have been constructed from *ab initio* CI one- and two-electron density matrices for the homonuclear diatomic molecules Li_2, N_2, F_2. The structure of v_{xc} has been analyzed in terms of its components $v_{\mathrm{xc}}^{\mathrm{hole}}$, $v_{c,\mathrm{kin}}$, and v_{resp}. The bond formation manifests itself in a plateau in $v_{\mathrm{xc}}^{\mathrm{hole}}$ in the bonding region of Li_2 and N_2, a bond midpoint peak in v_{resp} for N_2 and F_2, and a bond midpoint peak in $v_{c,\mathrm{kin}}$ for F_2. The combination of these features determines the form of v_{xc}. The relation of these features with various effects of electronic structure and electron correlation has been discussed.

The structure of $\varepsilon_{\mathrm{xc}}$ has been analyzed in terms of its exchange ε_x and correlation ε_c components. The latter component displays a sharp structure with intershell peaks and, in the case of N_2 and F_2, a bond midpoint peak, which has been related to left-right correlation. The exchange energy density ε_x is relatively smooth with a well around the nucleus, Coulombic asymptotics in the outer region, and a plateau in the bonding region.

We have compared the local behavior of the constructed ε_x and ε_c with that of the GGA exchange functionals of Becke, ε_x^B, and of Perdew and co-workers, $\varepsilon_x^{\mathrm{PW}}$, and with the correlation functionals of Perdew and co-workers, $\varepsilon_c^{\mathrm{PW}}$, and of Lee, Yang, and Parr, $\varepsilon_c^{\mathrm{LYP}}$, as well as with that of the corresponding LDA functionals. LDA tends to underestimate exchange and to overestimate correlation. In particular, the LDA correlation energy density $\varepsilon_c^{\mathrm{LDA}}$ is both highly overattractive and structureless as compared to ε_c. The gradient corrections create a considerable amount of structure for the correlation functions $\varepsilon_c^{\mathrm{GGA}}$ and bring the GGA exchange functions $\varepsilon_x^{\mathrm{GGA}}$ closer to ε_x. Still, the the $\varepsilon_x^{\mathrm{GGA}}$ show appreciable local deviations from ε_x and significant local differences in the comparison between the $\varepsilon_c^{\mathrm{GGA}}$ and ε_c have been found. The latter cannot be required to coincide, given the nonuniqueness of the correlation energy density, but for the former close correspondence is expected (at least for GGA of Becke) since the GGA exchange energy density tries to model the exchange hole potential which we use as exact ε_x.

The gradient corrections also bring the GGA exchange and correlation energies much closer to the KS exchange energy E_x and to the empirical estimate E_c^{emp} of the true correlation energy, respectively. For N_2 and F_2 they seem to overcorrect and the GGA exchange energies are consistently too large (too negative) as compared to E_x, while the GGA correlation energies are too small as compared to E_c^{emp}. However, the differences of opposite signs compensate each other and the resulting GGA exchange-correlation energies are rather close (especially, in the case of N_2) to the sum $(E_x+E_c^{\mathrm{emp}})$.

Concerning the systematic deviation between the GGA and KS exchange and correlation energies separately, we have noted that qualitative considerations concerning the behavior of Fermi and Coulomb holes in molecules on one hand and in the electron gas on the other, suggest that the LDA and GGA exchange functionals represent effectively not only exchange, but also the molecular nondynamical Coulomb correlation. At the same time the nondynamical correlation is not expected to be covered by the GGA correlation functionals, which represent the dynamical Coulomb correlation only. We have observed (cf. also [36]), using *ab initio* nondynamical correlation energies E^{nd}, that the integrated GGA exchange and correlation energies provide semiquantitative evidence for this point of view. In the present work we have demonstrated that the local behavior of the GGA exchange and correlation energies provides qualitative support for this point of view. Addition of the difference between the GGA and KS exchange energy densities, which supposedly mimics nondynamical correlation, to the GGA correlation energy density, does give qualitative improvement notably in the bonding region towards the KS ε_c.

[1] W. Kohn, A. D. Becke, and R. G. Parr, J. Phys. Chem. **100**, 12 974 (1996).

[2] R. Van Leeuwen, O. V. Gritsenko, and E. J. Baerends, in *Density Functional Theory I*, edited by R. F. Nalewajski, Topics in Current Chemistry Vol. 180 (Springer-Verlag, Berlin, 1996), p. 107.

[3] C. O. Almbladh and A. C. Pedroza, Phys. Rev. A **29**, 2322 (1984).

[4] F. Aryasetiawan and M. J. Stott, Phys. Rev. B **34**, 4401 (1986).

[5] Q. Zhao, R. C. Morrison, and R. G. Parr, Phys. Rev. A **50**, 2138 (1994).

[6] R. van Leeuwen and E. J. Baerends, Phys. Rev. A **49**, 2421 (1994).

[7] R. C. Morrison and Q. Zhao, Phys. Rev. A **51**, 1980 (1995).

[8] O. V. Gritsenko, R. van Leeuwen, and E. J. Baerends, Phys. Rev. A **52**, 1870 (1995).

[9] P. Süle, O. V. Gritsenko, R. van Leeuwen, and E. J. Baerends, J. Chem. Phys. **103**, 10 085 (1995).
[10] O. V. Gritsenko, R. van Leeuwen, and E. J. Baerends, J. Chem. Phys. **104**, 8535 (1996).
[11] A. C. Pedroza, Phys. Rev. A **33**, 804 (1986).
[12] C. J. Umrigar and X. Gonze, Phys. Rev. A **50**, 3827 (1994).
[13] O. V. Gritsenko, R. Van Leeuwen, and E. J. Baerends, Int. J. Quantum Chem. **61**, 231 (1997).
[14] S. Lundqvist and N. H. March, *Theory of the Inhomogeneous Electron Gas* (Plenum, New York, 1983).
[15] J. P. Perdew, K. Burke, and Y. Wang, Phys. Rev. B **54**, 16 533 (1996).
[16] C. F. Fischer, *The Hartree-Fock Method for Atoms* (Wiley, New York, 1977).
[17] J. B. Lagowski and S. H. Vosko, J. Phys. B **21**, 203 (1988).
[18] E. R. Davidson, S. A. Hagstrom, S. J. Chakravorty, V. M. Umrigar, and C. F. Fischer, Phys. Rev. A **44**, 7071 (1991).
[19] S. J. Chakravorty, S. R. Gwaltney, E. R. Davidson, F. A. Parpia, and C. F. Fischer, Phys. Rev. A **47**, 3649 (1993).
[20] A. D. Becke, J. Chem. Phys. **96**, 2155 (1992).
[21] A. D. Becke, J. Chem. Phys. **97**, 9173 (1993).
[22] A. Becke, Phys. Rev. A **38**, 3098 (1988).
[23] J. P. Perdew, in *Electronic Structure of Solids*, edited by P. Ziesche and H. Eschrig (Akademie Verlag, Berlin, 1991), pp. 11–20.
[24] J. P. Perdew, J. A. Chevary, S. H. Vosko, K. A. Jackson, M. R. Pederson, D. J. Singh, and C. Fiolhais, Phys. Rev. B **46**, 6671 (1992).
[25] C. Lee, W. Yang, and R. G. Parr, Phys. Rev. B **37**, 785 (1988).
[26] M. A. Buijse, E. J. Baerends, and J. G. Snijders, Phys. Rev. A **40**, 4190 (1989).
[27] C. Huang and C. J. Umrigar, Phys. Rev. A **56**, 290 (1997).
[28] G. Hunter, Int. J. Quantum Chem. **9**, 237 (1975).
[29] P. R. T. Schipper, O. V. Gritsenko, and E. J. Baerends, Theor. Chem. Accounts **98**, 16 (1997).
[30] D. C. Langreth and J. P. Perdew, Solid State Commun. **17**, 1425 (1975).
[31] O. Gunnarsson and B. I. Lunqvist, Phys. Rev. B **13**, 4274 (1976).
[32] O. V. Gritsenko, R. van Leeuwen, and E. J. Baerends, J. Chem. Phys. **101**, 8955 (1994).
[33] V. R. Saunders and J. H. van Lenthe, Mol. Phys. **48**, 923 (1983).
[34] G. C. Lie and E. Clementi, J. Chem. Phys. **60**, 1275 (1974).
[35] D. E. Woon and T. H. Dunning, J. Chem. Phys. **103**, 4572 (1995).
[36] O. V. Gritsenko, P. R. T. Schipper, and E. J. Baerends, J. Chem. Phys. **107**, 5007 (1997).
[37] M. A. Buijse, Ph.D. thesis, Vrije Universiteit, Amsterdam, 1991.
[38] M. A. Buijse and E. J. Baerends, in *Electronic Density Functional Theory of Molecules, Clusters and Solids*, edited by D. E. Ellis (Kluwer Academic Publishers, Dordrecht, 1995), pp. 1–46.
[39] R. van Leeuwen, O. V. Gritsenko, and E. J. Baerends, Z. Phys. D **33**, 229 (1995).
[40] O. V. Gritsenko, R. van Leeuwen, E. van Lenthe, and E. J. Baerends, Phys. Rev. A **51**, 1944 (1995).
[41] J. D. Talman and W. F. Shadwick, Phys. Rev. A **14**, 36 (1976).
[42] K. Aashamar, T. M. Luke, and J. D. Talman, At. Data Nucl. Data Tables **22**, 443 (1978).
[43] J. D. Talman, Comput. Phys. Commun. **54**, 85 (1989).
[44] J. B. Krieger, Y. Li, and G. J. Iafrate, Phys. Rev. A **45**, 101 (1992).
[45] A. Savin, H. Stoll, and H. Preuss, Theor. Chim. Acta **70**, 407 (1986).
[46] J. P. Perdew and Y. Wang, Phys. Rev. B **45**, 13 244 (1992).
[47] B. Miehlich, A. Sowin, H. Stoll, and H. Preuss, Chem. Phys. Lett. **157**, 200 (1989).
[48] H. Stoll, C. M. E. Pavlidou, and H. Preuss, Theor. Chim. Acta **49**, 143 (1978).
[49] O. V. Gritsenko, R. van Leeuwen, and E. J. Baerends, Int. J. Quantum Chem. **60**, 1375 (1996).
[50] J. C. Slater, *Quantum Theory of Molecules and Solids* (McGraw-Hill, New York, 1974), Vol. 4.
[51] M. Cook and M. Karplus, J. Phys. Chem. **91**, 31 (1987).
[52] V. Tschinke and T. Ziegler, J. Chem. Phys. **93**, 8051 (1990).